

A numerical study on the role of leakage distribution and internal leakages under unsteady wind conditions

Dimitrios Kraniotis*, Tormod Aurlien, Thomas Kringlebotn Thiis

Department of Mathematical Sciences and Technology, Norwegian University of Life Sciences

Drøbakveien 31, P.O. box: 5003, IMT, N-1423, Ås, Norway

**Corresponding author: dimitrios.kraniotis@umb.no*

ABSTRACT

The existence of air leakages in a building has been very clearly stated as an important reason for energy loss. The decrease in the efficiency of the mechanical ventilation has also been clarified. The global demand for achieving nearly zero-energy buildings makes the uncontrolled leakage paths even more undesired. Despite the fact that steady state measurements of in- and exfiltration rates offer a simple and easy way of estimating the airtightness level of an enclosure, a supplement to those methods might be imposed.

While a significant amount of studies points out the key role of the ‘artificial’ unsteady conditions to the actual leakage rates of a building, there are only few that discuss the influence of natural unsteady phenomena. In this context, the correlation between the dynamic characteristics of the wind and the leakage numbers of a building, should be more studied. Computational Fluid Dynamics (CFD) could be employed in order to investigate the role of the air flow mechanisms.

In the current numerical study, unsteady wind conditions are performed around an one-storey building-model of size 5m x 10m x 3m. Variable leakage areas A_{leak} around windows are simulated and solved in a transient mode aiming to investigate the role of the distribution of the leakages under natural conditions. A ratio ($0 \leq \alpha \leq 1$) that represents the portion of leakages (distribution) per surface is employed and the infiltration rates respect to this ratio are shown. Different situations of the enclosure volume (from the perspective of internal wall airtightness) are assumed in order to investigate the influence of the latter to the infiltration rate of the building’s envelope. The impact of the internal leakages is proven and the importance of controlling them is discussed.

KEYWORDS

Leakage rate, air flow, air infiltration, leakage distribution, internal leakages, unsteady wind conditions, wind gust, computational fluid dynamics, shear-stress-transport

INTRODUCTION

Air infiltration has been recognized as one of the major reasons for energy loss [1]. The decrease in the efficiency of the mechanical ventilation has also been clarified [2]. Uncontrolled leakage paths have very clearly stated as pervasive, resulting in severe consequences [3]. The nature and extent of uncontrolled air flow have also been studied through testing, measurement and monitoring. Many researchers have also stated the uncertain phenomena that are connected to the airflow through leakages located on a building envelope. The dynamic characteristics of air infiltration have been pointed [4] and therefore challenges arise upon that field. The role of the climate parameters and location characteristics on average infiltration rates has also been studied [5]. Turbulence causing wind gustiness is recognized as one major factor that affects infiltration [6]. In addition, building aerodynamics contributes to air infiltration too. In that context, modelling approaches have been presented [7], [8]. Although, the air leakage of a building envelope can

be determined from fan pressurization measurements with a blower door, estimating in a simple and easy way an enclosure's airtightness level [9], further research that takes the latter phenomena into account should be done.

Furthermore, leakage distribution has been mentioned as important factor towards the annual infiltration rate calculation [10]. Models have been developed towards the estimation of leakage distribution [11]. In addition, the latter affects even the air pressure conditions in building and the wind-induced internal pressure fluctuations [12], [13]. In the same manner, the role of internal volume has been mentioned [14] as well as the influence of internal air leakages [15].

Computational fluid dynamics (CFD) could be employed to investigate the role of the air flow mechanisms from the perspective of the phenomena presented above, especially under unsteady conditions. Numerical studies could contribute to an estimation of the impact of potential leakages areas in the building envelope as well as in internal elements. Facing the global demand for achieving nearly zero-energy buildings, a more holistic and detailed approach of the phenomena linked to air infiltration should be given through both measurements and numerical simulations.

CASE STUDY

The current numerical study deals with the influence of unsteady wind to the instantaneous infiltration (exfiltration) rates of an one-storey building-model (of size 5m x 10m x 3m) on which variable leakage areas around windows are simulated. Two 'windows' are used on each side. The size of each 'window' is 0,8m x 0,8m. The leakages are supposed to be 'cracks' along their frame. The total leakage area (whole building-model) is assumed to be 64cm².

The leakages are located on the windward and on the leeward side of the model. Seven different cases of distribution (windward vs leeward) are solved. For the representation of the latter, a ratio α is defined as follows:

$$\alpha = \frac{A_{leak,front}}{A_{leak,total}} * 100 [\%] \quad (1)$$

where

$A_{leak,front}$: the leakages located on the windward side (front side) for the building-model, expressed in cm² and

$A_{leak,total}$: the total leakage area of the model in cm² (both on windward and leeward sides), which as mentioned above equals 64cm².

In fact, the ratio α expresses the leakages located on the windward side as fraction to the total leakage areas of the building. The α takes the values: $\alpha = 5$, $\alpha = 15$, $\alpha = 30$, $\alpha = 50$, $\alpha = 70$, $\alpha = 85$ and $\alpha = 95$ [%]. To give a magnitude of order of the amount of the leakages:

$$\frac{A_{leak,total}}{total\ model\ surface} = 4,57 * 10^{-5} \quad (2)$$

Furthermore, since the influence of wind gust frequency ω has been discussed (especially for single-side airflow) [14], studying of its connection to the leakage distribution would be useful. Thus, two different gust frequencies are assumed, ω_{high} and ω_{low} and they are implemented in the wind profile formula as a sinusoidal factor (explained in the 'methodology').

Finally, three different 'situations' (S_1 , S_2 , S_3) regarding the internal volume are simulated in order to research the influence of the internal leakages and their connection the external ones. The first case S_1 refers to an internal volume without internal walls ('uniform', single space)

(fig. 1). The second and the third cases (S_2 and S_3 respectively) both assume the existence of internal wall that divide the whole space in two ‘rooms’. The difference is that in S_2 a leakage area of 4cm^2 is assumed to be located on the low level of the wall, allowing the inter-flow between the two rooms (fig. 3a and 3b), while in S_3 there are not internal leakages at all (assumption of completely tight internal wall) (fig. 2).

Summarizing, 42 cases are studied in total:

$$\Sigma = 7(\text{leakage distribution cases}) * 2(\text{wind gust frequency cases}) * 3(\text{internal space cases}).$$

A notation described by the following rule is employed and used hereinafter:

(Internal volume case S_i) - (leakage distribution α_j) - (frequency of the wind gust ω_k),

where:

- $i = 1, 2 \text{ or } 3,$
- $j = 5, 15, 30, 50, 70, 85 \text{ or } 95 \text{ and}$
- $k = \text{‘high’ or ‘low’}.$

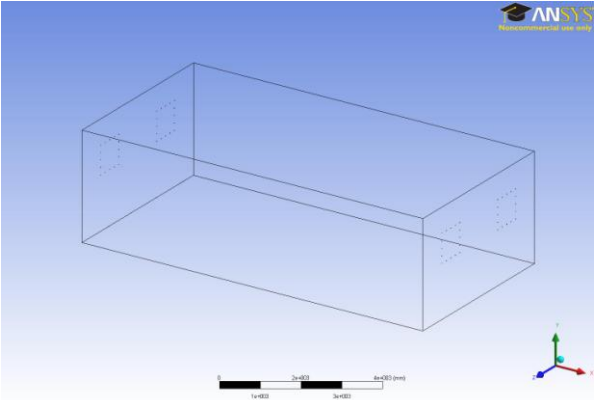


Figure 1. The case S_1 : ‘uniform’ single space (no internal wall).

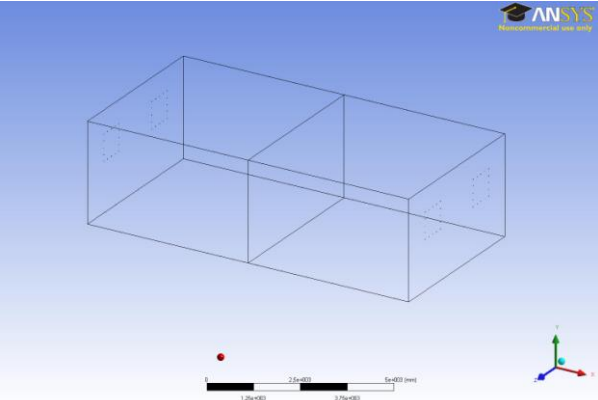


Figure 2. The case S_3 : two spaces separated by an internal wall. No internal leakages.

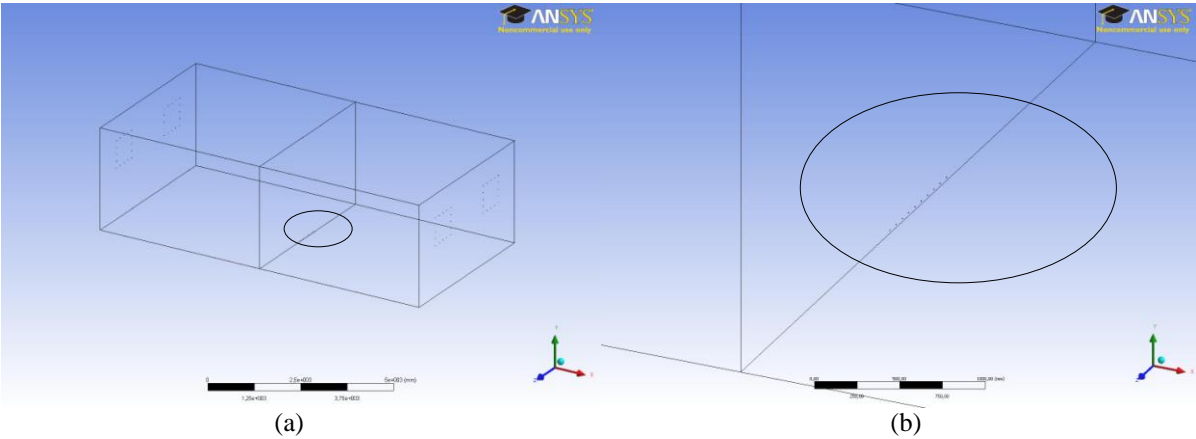


Figure 3. The case S_2 : two spaces separated by an internal wall. Internal leakages are located on the low level of the wall (circle area).

The table 1 shows, as example, the notation for leakage distribution of $\alpha = 5\%$ and $\alpha = 70\%$ for all the subcases of the internal volumes (and in the high gust frequency).

Case	Internal volume	Leakage distribution	Wind gust frequency
$S_1-\alpha_5-\omega_{high}$	'uniform' space	$\alpha = 5\%$	high
$S_2-\alpha_5-\omega_{high}$	two spaces – with internal leakages	$\alpha = 5\%$	high
$S_3-\alpha_5-\omega_{high}$	two spaces – no internal leakages	$\alpha = 5\%$	high
$S_1-\alpha_{70}-\omega_{high}$	'uniform' space	$\alpha = 70\%$	high
$S_2-\alpha_{70}-\omega_{high}$	two spaces – with internal leakages	$\alpha = 70\%$	high
$S_3-\alpha_{70}-\omega_{high}$	two spaces – no internal leakages	$\alpha = 70\%$	high

Table 1. Example of the notation followed. Here, the notations for the leakage distribution $\alpha = 5\%$ and $\alpha = 70\%$ in the high gust frequency ω_{high} .

METHODOLOGY

The CAD model was developed in ANSYS Design ModelerTM 12.1. The CFX-mesh method of the ANSYS Mesh program (involved in ANSYS Workbench) was employed for committing the meshes (fig. 4). The fluid dynamic package ANSYS CFX 14.0 was used as solver for the numerical simulations. Pressure distribution around a building is in general important to get correct prediction of the pressure gradients and consequently of the air infiltration through the envelope. Among the available turbulence models, the Shear-Stress-Transport (SST) model, a two equation $k-\omega$ based model [16], was imposed. The reason for that is the inclusion of transport effects into the formulation of the eddy-viscosity. This results in a major improvement in terms of flow separation predictions [17]. In addition, other relevant studies have shown a good agreement between SST model and full scale data, better rather than compared with standard $k-\varepsilon$ and RNG $k-\varepsilon$ models [18].

A period of 30sec was assumed to be the total time per run, while a fine timestep of 0,25sec was selected. At the inlet of the domain, a logarithmic wind profile was assumed based on the equation (fig. 5):

$$\frac{u}{u_*} = \frac{1}{\kappa} \ln\left[\frac{z}{z_0} - \Psi_m\left(\frac{z}{L}\right)\right] + 2\sin(2\pi\omega t) \quad (3)$$

where u is the wind velocity at height z , u_* is the shear velocity, κ von Karman's constant, z_0 the roughness length and Ψ_m a stability function. The stability function can be evaluated directly from the Monin and Obukhov length L , knowing the flux of sensible heat, or indirectly through simultaneous measurements of air temperature profiles [19]. Under neutral stability conditions Ψ_m and $\frac{z}{L}$ vanish. The second term in the right side of the wind profile represents the wind gustiness frequency ω .

As mentioned above, two different gust frequencies ω have been employed, $\omega_{high} = 0,5Hz$ corresponds to the high frequency and $\omega_{low} = 0,1 Hz$ to the low one (fig. 6). Thus, the period of the wind velocity on a certain height is $T_{high} = 2sec$ and $T_{low} = 10sec$ respectively.

The leakage area along each window side represents a 'crack' of 0,8m long, simulated by a row of 5 circular 'holes'. The latter are equally distributed along the window side and their total 'opening area' equals the the leakage area of the relevant crack.

The instantaneous mass flow rate Q_m is solved numerically and extracted. Thus, the instantaneous volumetric flow rates Q_v across the leakage areas are calculated (based on the transient, local density field) for the interval run time (30sec) for every case. Assuming that

the dynamic mathematical and physical behavior of the model does not change within an hour, the equivalent air change rate ΣACH_i extrapolated over time $t_{tot} = 1h$ is calculated:

$$\Sigma ACH_i = \frac{3600}{t_{run}} * \frac{\left(\int_0^{t_{run}} Q_v dt\right)}{V} \quad (4)$$

where

t_{run} is the total run time per case, means $t_{run} = 30sec$ and V the volume of the enclosure.

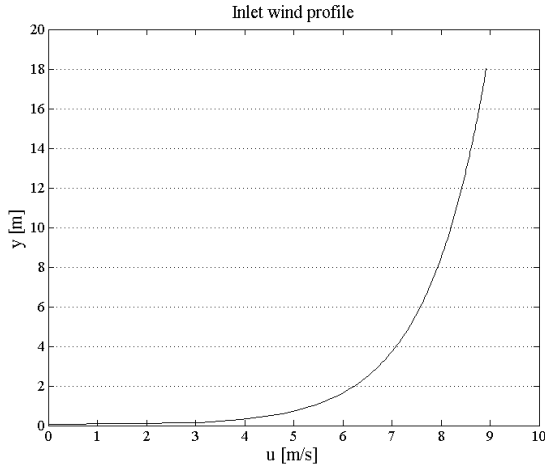


Figure 5. The selected inlet wind profile.

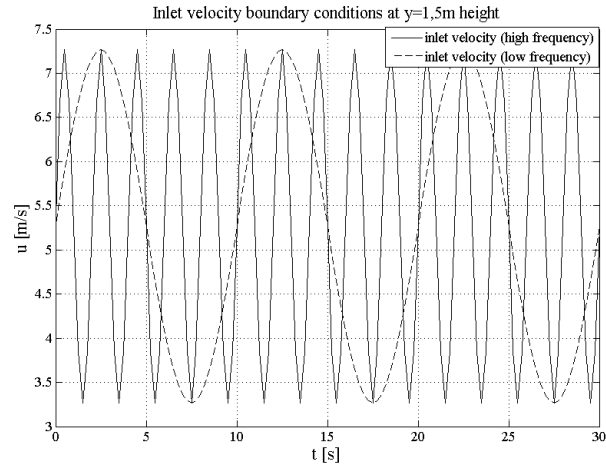


Figure 6. Inlet velocity boundary conditions at the height of $y = 1,5m$ as they have been defined for the high frequency ω_{high} and the low ω_{low} .

RESULTS

The equivalent air change rates ΣACH_i for all the cases S_1 , S_2 and S_3 are plotted against the leakage ratio α and shown in figures 7, 9 and 12 respectively. In each graph, two lines appear representing the rates under high and low wind gust frequency.

In the figure 7, it is clear that the strong ‘cross ventilation’ that takes place in the case of the single space results to relatively very high infiltration rates. Especially under the conditions of the high frequency gustiness the air exchange becomes even more severe. Having employed the assumption of ‘one room’ with no internal wall, there are no serious resistance against the flow. The ΣACH_i increases respect to the ratio α , and appears the maximum value when the leakages are equally distributed on the windward and leeward façade of the model ($\alpha = 50\%$). The air change rates seem to get lower again when α increases more. The role of the inertia forces of the enclosure appear to be in general weak in the case S_1 . However, it would be reasonable to claim that when the leakages are mostly located either on the windward or on the leeward side (the ΣACH_i seems to have fairly symmetric picture), the compressibility of the volume tends to reduce the actual leakage rates, as the model behavior is getting more similar to single-side infiltration (fig. 8).

In the case of S_2 the existence of a relatively tight internal wall (the internal leakages are only 6,25% of the leakages of the envelope) seems to have a dramatic impact (drop) to the air change rates (fig. 9). The ΣACH_i appear (for both the gust frequencies ω_{high} and ω_{low}) to be much lower. Although a ‘cross ventilation’ takes place even in this case, the quite high level of tightness of the interior element ‘activates’ the inertia forces of the enclosure, resulting to lower infiltration rates. Especially for the high wind gustiness, it seems that the most

unbalanced the leakage distribution, the lowest the infiltration (exfiltration) rates that are caused. When the gustiness of wind is getting more mild (ω_{low}), the influence of the relatively

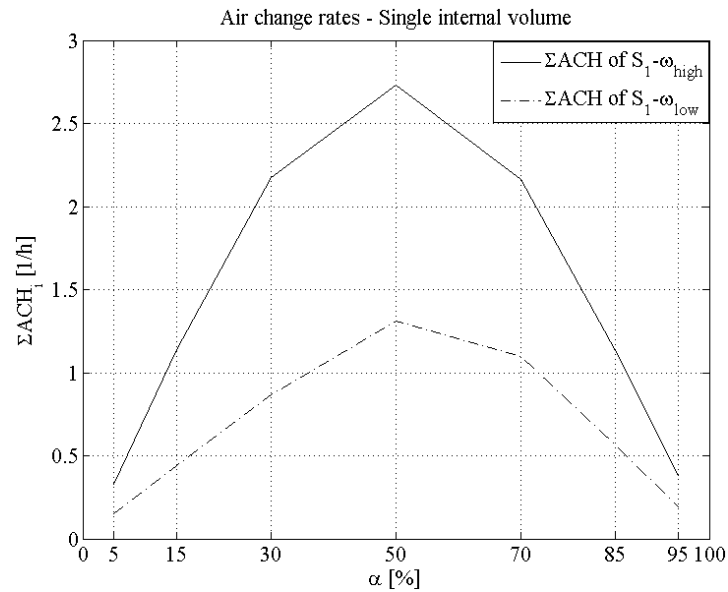


Figure 7. The air change rate for the case of the ‘single space’.

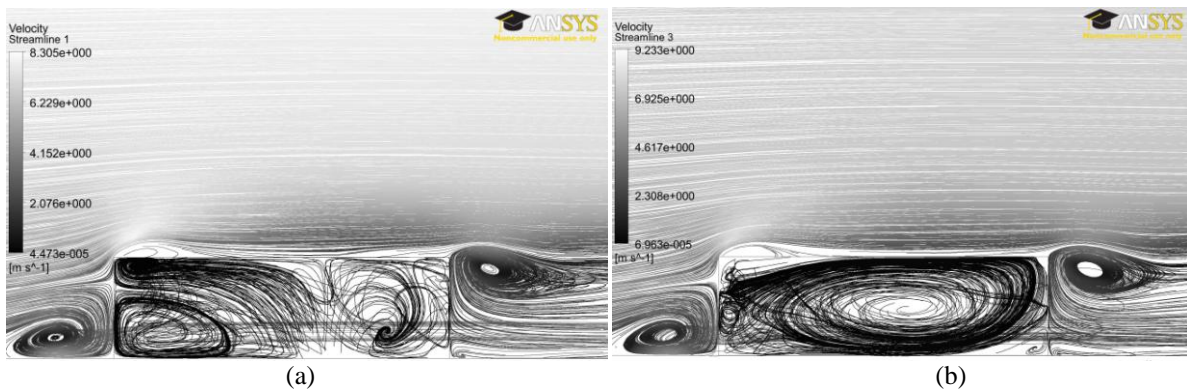


Figure 8. The velocity steamlines using a symmetry plane (timestep : $t = 2s$). (a) case of $S_1-\alpha_{95}-\omega_{high}$, (b) case of $S_1-\alpha_{30}-\omega_{high}$.

tight wall is becoming even more significant, resulting in air change rates within the acceptable range, as described in building regulations [20].

However, a difference can be pointed out when comparing the cases of high and low frequency. Under ω_{high} , the infiltration rate of $S_2-\alpha_5-\omega_{high}$ is higher than the ‘inverse’ case of $S_2-\alpha_{95}-\omega_{high}$, as well as $S_2-\alpha_{15}-\omega_{high} > S_2-\alpha_{85}-\omega_{high}$, as well as $S_2-\alpha_{30}-\omega_{high} > S_2-\alpha_{70}-\omega_{high}$. In contrast, in the low wind frequency ω_{low} , higher air change rates appear as result of leakage concentration mostly on the windward side. The flow patterns in figure 10(a) show a mild air circulation during ω_{high} even when the size of the leakages on windward is relatively big. The reason could be the size of the internal leakages compared to the external ones on the leeward façade; when they have the same magnitude of order, the inertia forces of the ‘second room’ seem to increase, preventing the air to flow from the ‘first room’, even though there is a significant amount of air that enters from the environment to the latter. But when the leeward leakage areas are getting larger, the pressure field in the ‘second room’ changes, forcing the air to flow out through them.

In case the unsteady wind is more mild (low frequency), the size of the ‘inlet’ on windward dominates the airflow (fig. 11). The reason could be that the wind gusts are not anymore so

strong enough in this case that they would force great amount of air to flow to the ‘second room’, which remains more ‘neutral’ compared to the ‘first room’.

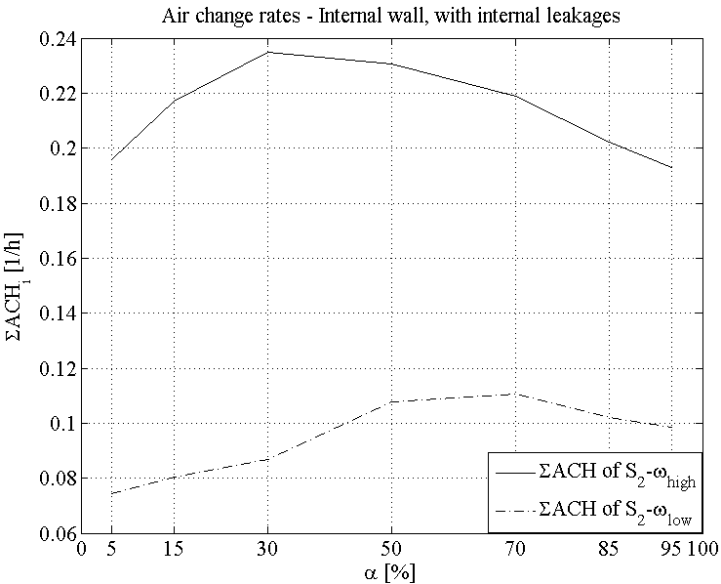


Figure 9. The air change rate for the case of the two rooms, separated by an internal wall where leakages are located on.

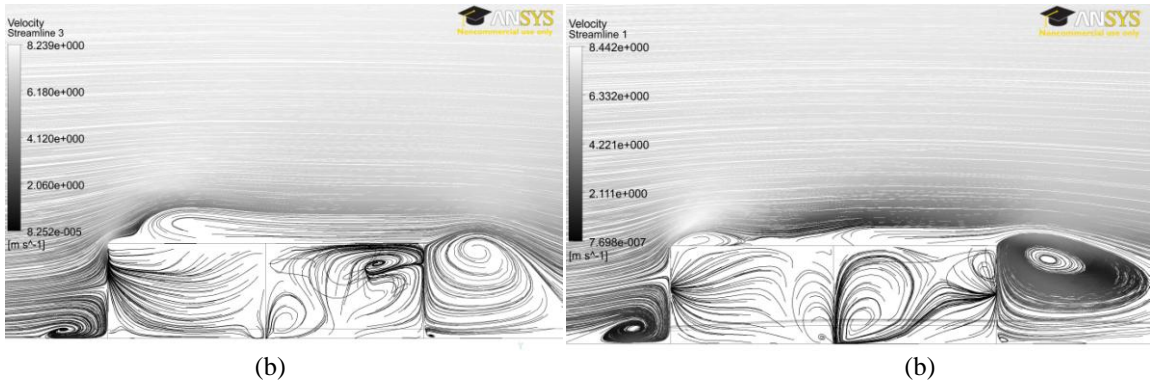


Figure 10. The velocity streamlines using a symmetry plane (timestep : $t = 2s$). (a) case of $S_2-\alpha_{95}-\omega_{high}$, (b) case of $S_2-\alpha_{30}-\omega_{high}$.

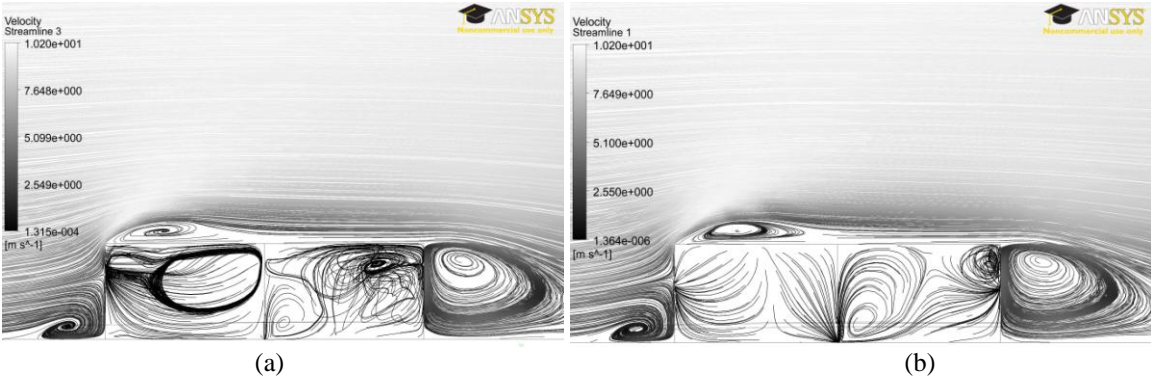


Figure 11. The velocity streamlines using a symmetry plane (timestep : $t = 3s$). (a) case of $S_2-\alpha_{95}-\omega_{low}$, (b) case of $S_2-\alpha_{05}-\omega_{low}$.

The role of the internal leakages is even more clearly shown in the figure 12 that represents the situation S_3 . Assuming that the internal wall is completely tight, the air change rates seem to become even lower compared to S_2 highlighting the importance of controlling the internal

leakage paths. Furthermore, reading the infiltration rates from the perspective of the blower door ‘rule-of-thumb’ ($ACH_{50} = \Sigma ACH_i * 20$), they fulfil requirements of a ‘passive house airtightness level’ [21]. The inertia forces of the first ‘room’ are in this case higher because of the single-side infiltration and the compressibility of the volume decreases. The second ‘room’ has gotten ‘isolated’ in this case, so there is not significant air exchange through the leeward leakages. Thus, the most favorable case seems to be when the leakages are mostly concentrated on this façade (α_{05} - leeward).

The ΣACH_i increases with the ratio α in both the wind frequencies studied. The maximum value appears when the leakage area on windward is getting big enough (α_{95}).

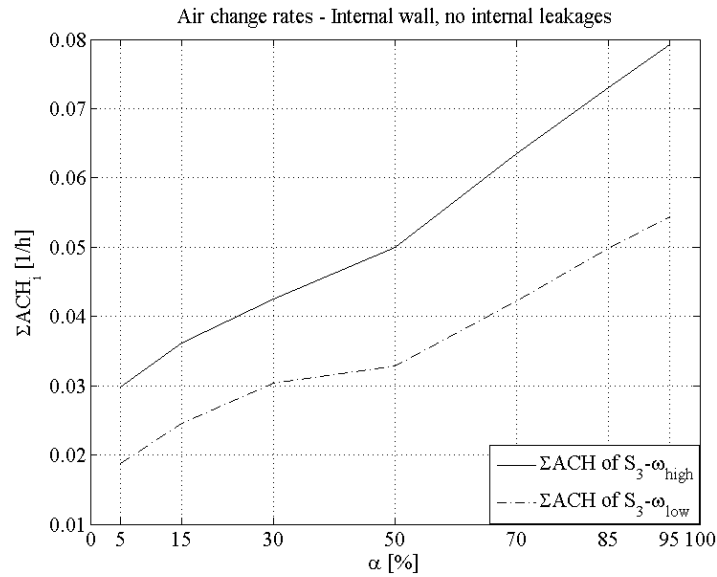


Figure 12. The air change rate for the case of the two rooms, separated by a totally tight internal wall.

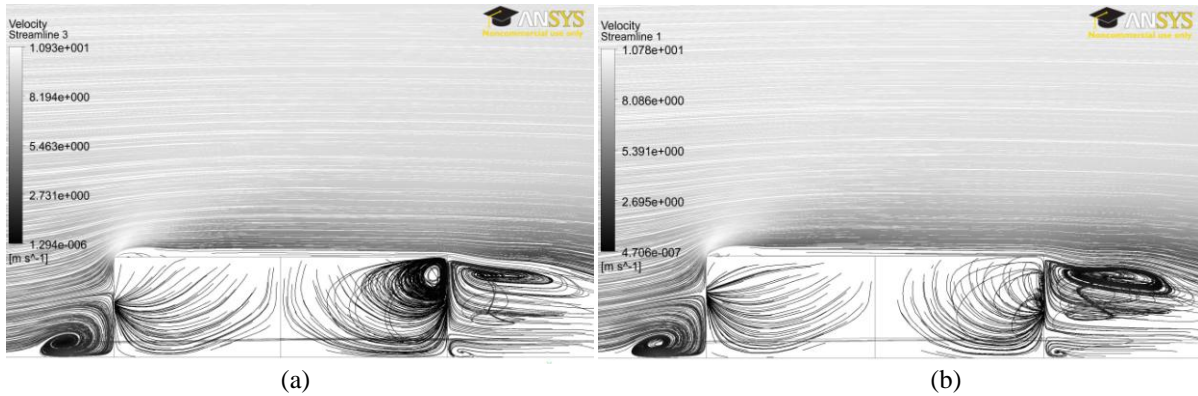


Figure 13. The velocity streamlines using a symmetry plane (timestep : $t = 3s$). (a) case of $S_3-\alpha_{05}-\omega_{high}$, (b) case of $S_3-\alpha_{95}-\omega_{high}$.

In all the cases (S_1 , S_2 and S_3), the impact of the gust frequency ω_i seems to be very important resulting to increased infiltration rates. The normalized difference δ between the air exchanges during the high frequency ω_{high} and those during the low one ω_{low} is drawn against the ratio α [fig. 14].

$$\delta = \frac{\Delta(\Sigma ACH_{high} - \Sigma ACH_{low})}{\Sigma ACH_{low}} \quad (5)$$

In the figure 14, it is clear that the influence of wind gustiness, in both the cases S_1 (single space) and S_2 (internal wall with leakages), is more significant compared to the case S_3

(completely tight internal wall). Again, increasing the tightness of the internal elements, the impact of the wind unsteadiness becomes less important. In addition, in the first cases the normalized difference δ has similar behavior, showing that higher wind gustiness results to even higher infiltration rates when most leakages are concentrated on the windward façade. In contrast, in case S_3 (internal wall with no leakages), the increase of wind frequency has similar results to the ΣACH_i in the whole range of the leakage distribution that is studied. The dynamic characteristics of the wind and the inertia of the enclosure mass seem to influence in an analogue manner the actual air change rates.

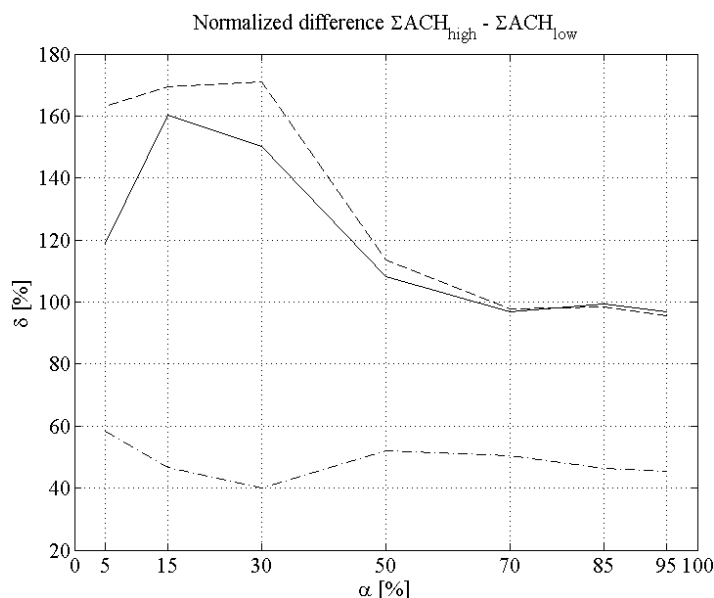


Figure 14. The normalized difference δ between the air exchanges under the high frequency ω_{high} and those under the low frequency ω_{low} is drawn against the ratio α .

CONCLUSION

An one-storey building-model with variable leakage areas on the windward and the leeward side was simulated and studied numerically under unsteady wind conditions. Two wind gust frequencies ($\omega_{high} = 0,5Hz$ and $\omega_{low} = 0,1Hz$) were used to describe the inlet boundary conditions. A ratio α [%] ($5\% < \alpha < 95\%$) was employed to describe the leakages located on the windward side as fraction to the total leakage areas of the building. Three different situations of the internal volume were assumed; a single space (S_1), an enclosure with an internal wall with leakages (S_2) and an enclosure similar to the latter but without internal leakages (S_3).

In total 42 cases were solved using the shear-stress turbulent model (SST). The equivalent air change rate ΣACH_i , extrapolated over time $t_{tot} = 1h$, was calculated and was shown against the leakage distribution α . The leakage distribution seems to govern the infiltration rates in case of a strong cross 'ventilation' (S_1). The most severe situation appears to be when the leakages areas on the windward and the leeward façade are of the same magnitude of order. Again, the most 'unbalanced' the way that the leakages are distributed the least air exchanges that take place.

Existence of relatively tight internal walls (S_2) decrease dramatically the leakage numbers. Even though a 'cross ventilation' takes place even in this case, the quite high level of tightness of the interior element 'activates' the inertia forces of the enclosure (of the 'front' room). Fullfilling high tightness of the internal elements (S_3), the air change rates decrease even more, reaching almost passive house airtightness standards (even under more severe

wind gustiness). In addition, in the latter case, it seems to be of relatively high importance to eliminate as possible the leakages on the windward façade (according to the main wind direction of a location).

It would be reasonable to claim that internal leakages seems to be a major parameter towards the demand of decreasing the infiltration rates. Gustiness of wind is also a critical factor that results to higher leakage numbers. However, increasing the tightness of the internal elements, the impact of the wind unsteadiness becomes less severe. To determine even further the influence of wind frequency, a graph that represents the normalized difference between ΣACH_{high} and ΣACH_{low} is defined and is shown against the ratio α .

The study sets up issues regarding the uncontrolled leakages on the building envelope. The detection of leakages and their distribution should might be considered as critical factor. Furthermore, internal leakages seem to play an important role towards the nearly-energy-zero building target. Further research needs to be done, in order to investigate the connection between internal and external leakages in a detail way.

REFERENCES

- [1] Shaw C.-Y. 1981. *A correlation between air infiltration and air tightness for houses in a developed residential area*, National Research Council Canada, Ottawa.
- [2] Månsson L.G. 2002. *IEA ECBCS Annex 27 – Evaluation and demonstration of domestic ventilation systems – Simplified tools Handbook*, FaberMaunsell Ltd, United Kingdom.
- [3] Cummings J.B., Withers C.R., Moyer N., Fairey P., McKendry B. 1996. *Uncontrolled air flow in non-residential buildings – Final report*, Florida Energy Office - Department of Community Affairs, Tallahassee, Florida.
- [4] Hill J.E., Kusuda T. 1975. *Dynamic characteristics of air infiltration*, ASHRAE Trans. 81 (1) 168–185, ASHRAE, New York.
- [5] Sherman M. H. 1986. *Estimation of infiltration from leakages and climate indicators*, Energy and buildings Vol. 10, 81–86.
- [6] Haghighat F., Brohus H., Rao J. 1999. *Modelling air infiltration due to wind fluctuations – a review*, Building and environment Vol. 35, 377–385.
- [7] Haghighat F., Rao J., Fazio P. 1991. *The influence of turbulent wind on air change rates – a modelling approach*, Building and environment Vol. 26, 95–109.
- [8] Haghighat F., Rao J., Riberon J. 1992. *Modelling fluctuating airflow through large openings*, 13th AIVC conference, Nice, France.
- [9] Sherman M.H. 1995, *The use of blower-door data*, Indoor Air Vol. 5, 215–224.
- [10] Dubrul C. 1988. *Inhabitants behavior with respect to ventilation. Technical note 23*, Air infiltration and Ventilation Centre AIVC, pp. 63.
- [11] Chan W.R., Price P.N., Sohn M.D., Gadgil A.J. 2003, *Analysis of U.S. Residential Air Leakage Database*, LBNL Report Number 53367, Lawrence Berkeley National Laboratory, Berkeley, U.S.A.
- [12] Guha T.K., Sharma R.N., Richards P.J. 2011. *Internal pressure dynamics of a leaky building with a dominant opening*, Journal of Wind Engineering and Industrial Aerodynamics, Vol. 99, 1151-1161.
- [13] Kalamees, T., Korpi, M., Eskola, L., Kurnitski, J., Vinha, J. 2008. *The distribution of the air leakage places and thermal bridges in Finnish detached houses and apartment buildings*, Proceedings of the 8th Symposium on Building Physics in the Nordic Countries NSB2008, Copenhagen, 1095-1102.
- [14] Kraniotis D. Thiis T.K., Aurlien T., 2011. *Behavior of leakages exposed to dynamic wind loads. A numerical study using CFD on a single zone model*, Proceedings of the 32nd AIVC and 1st TightVent Conference, Brussels, Belgium, 80-82.

- [15] Aaltonen A., Lähdesmäki K., Vinha J. 2011, *Air tightness of structural elements and internal air leakages in a multi-apartment building*, Proceedings of the 9th Nordic Symposium on Building Physics NSB2011, Tampere, Finland, 79-86.
- [16] Menter F.R. 1994. *Two-equation eddy-viscosity turbulence models for engineering applications*, AIAA Journal, Vol. 32, no 8. 1598–1605.
- [17] ANSYS Inc. 2011. *ANSYS CFX-Solver Modeling Guide*, ANSYS CFX 14.0 help manual.
- [18] Guha, T.K., Sharma, R.N., Richards, P.J. 2009. *CFD modeling of wind induced mean and fluctuating external pressure coefficients on the Texas Technical University building*, EACWE 5.
- [19] Grimenes A.A., Thue-Hansen V. 2004. *Annual variation of surface roughness obtained from wind profile measurements*, Theoretical and Applied Climatology V. 79, 93-102.
- [20] Direktoratet for byggkvalitet 2010. *Byggteknisk forskrift – TEK 10, FOR 2010-03-26 nr 489: Forskrift om tekniske krav til byggverk (Byggteknisk forskrift)*, Oslo, Norway.
- [21] Feist W. 2010. *Active for more comfort – The Passive House*, International Passive House Association, Darmstadt, Germany.

